

Journal of Biomedical Optics

BiomedicalOptics.SPIEDigitalLibrary.org

Noninvasive measurement of glucose concentration on human fingertip by optical coherence tomography

Tseng-Lin Chen
Yu-Lung Lo
Chia-Chi Liao
Quoc-Hung Phan

SPIE.

Tseng-Lin Chen, Yu-Lung Lo, Chia-Chi Liao, Quoc-Hung Phan, "Noninvasive measurement of glucose concentration on human fingertip by optical coherence tomography," *J. Biomed. Opt.* **23**(4), 047001 (2018), doi: 10.1117/1.JBO.23.4.047001.

Noninvasive measurement of glucose concentration on human fingertip by optical coherence tomography

Tseng-Lin Chen,^a Yu-Lung Lo,^{a,b,*} Chia-Chi Liao,^a and Quoc-Hung Phan^a

^aNational Cheng Kung University, Department of Mechanical Engineering, Tainan, Taiwan

^bNational Cheng Kung University, Advanced Optoelectronic Technology Center, Tainan, Taiwan

Abstract. A method is proposed for determining the glucose concentration on the human fingertip by extracting two optical parameters, namely the optical rotation angle and the depolarization index, using a Mueller optical coherence tomography technique and a genetic algorithm. The feasibility of the proposed method is demonstrated by measuring the optical rotation angle and depolarization index of aqueous glucose solutions with low and high scattering, respectively. It is shown that for both solutions, the optical rotation angle and depolarization index vary approximately linearly with the glucose concentration. As a result, the ability of the proposed method to obtain the glucose concentration by means of just two optical parameters is confirmed. The practical applicability of the proposed technique is demonstrated by measuring the optical rotation angle and depolarization index on the human fingertip of healthy volunteers under various glucose conditions. © 2018 Society of Photo-Optical Instrumentation Engineers (SPIE) [DOI: [10.1117/1.JBO.23.4.047001](https://doi.org/10.1117/1.JBO.23.4.047001)]

Keywords: optical coherence tomography; differential Mueller matrix polarimetry; noninvasive glucose sensing.

Paper 170780RR received Dec. 4, 2017; accepted for publication Mar. 16, 2018; published online Apr. 10, 2018.

1 Introduction

With rising obesity levels around the world, diabetes has emerged as a major medical concern with significant health and economic implications. If left untreated, diabetes can result in blindness, kidney failure, loss of limbs, heart attacks, strokes, and even death.¹ Consequently, effective methods for diagnosing and monitoring diabetes are urgently required. Typically, such methods are based on measuring the glucose concentration in human blood or tissue. Noninvasive methods for glucose concentration determination either track an intrinsic molecular property of the glucose directly or the effects of glucose on the optical properties of the tissue or blood.² Methods of the former type typically track the optical rotation angle, near-infrared (NIR)/midinfrared absorption coefficient, Raman shift, or NIR photoacoustic absorption.^{3–5} By contrast, methods of the latter type generally measure parameters such as the light scattering coefficient of tissue, the refractive index of interstitial fluid, and the acoustic propagation speed in tissue.^{6–9} The optical measurements required for glucose determination are commonly performed using optical coherence tomography (OCT).^{10,11} For noninvasive glucose monitoring based on measurement of coherently scattered light from specific layers of tissues and slopes of OCT signals, Esenaliev et al.¹² showed that the slope of the OCT signal reduced substantially and linearly with increases in the blood glucose concentration. Larin et al.^{13,14} found that a good correlation exists between the OCT signal slope and the blood glucose concentration under normal physiological conditions. Kirillin et al.¹⁵ showed that the addition of glucose to 2% and 5% Intralipid suspension increased the refractive index and decreased the scattering coefficient, thereby leading to a reduction in the OCT signal slope. Additionally, various polarization-sensitive (PS) OCT structures

have been developed for measuring the depth-resolved optical birefringence properties of biological tissues using a Jones calculus formulation.^{16–18} Yao and Wang¹⁹ developed an enhanced PS-OCT system for measuring the full depth-resolved Mueller matrix of biological tissue. In a later study,²⁰ the same group used the PS-OCT system to measure the degree of polarization and backscattering coefficient of liquid and solid scattering samples. It was shown that the proposed system made possible the observation of several tissue structures that could not be visualized using a standard (nonpolarization) OCT setup. Liao and Lo²¹ proposed an OCT system based on a hybrid Mueller matrix formalism for extracting full-range measurements of the linear birefringence (LB) and linear dichroism (LD) properties of anisotropic optical samples. The results revealed that the proposed method was both more reliable and more accurate than traditional Mueller matrix decomposition methods.

Stokes–Mueller matrix polarimetry is a well-known technique for noninvasive diagnosis of cancerous tissue and turbid tissue-like scattering media.²² Phan and Lo²³ recently proposed a differential Mueller matrix polarimetry technique for performing noninvasive glucose monitoring on the human fingertip. In Ref. 23, samples were treated as a black box for simplicity. The circular birefringence (CB) and depolarization index of the human fingertip tissue were both found to vary with changes in the glucose concentration. Accordingly, the present study proposes a technique for extracting the CB and depolarization properties of glucose aqueous solutions using a Mueller OCT system. The feasibility of the proposed technique is demonstrated by measuring the CB and depolarization properties of glucose aqueous solutions with low scattering properties (i.e., 0.02% Lipofundin addition) and high scattering properties (i.e., 2% Lipofundin addition), respectively. Finally, the practical

*Address all correspondence to: Yu-Lung Lo, E-mail: loyl@mail.ncku.edu.tw

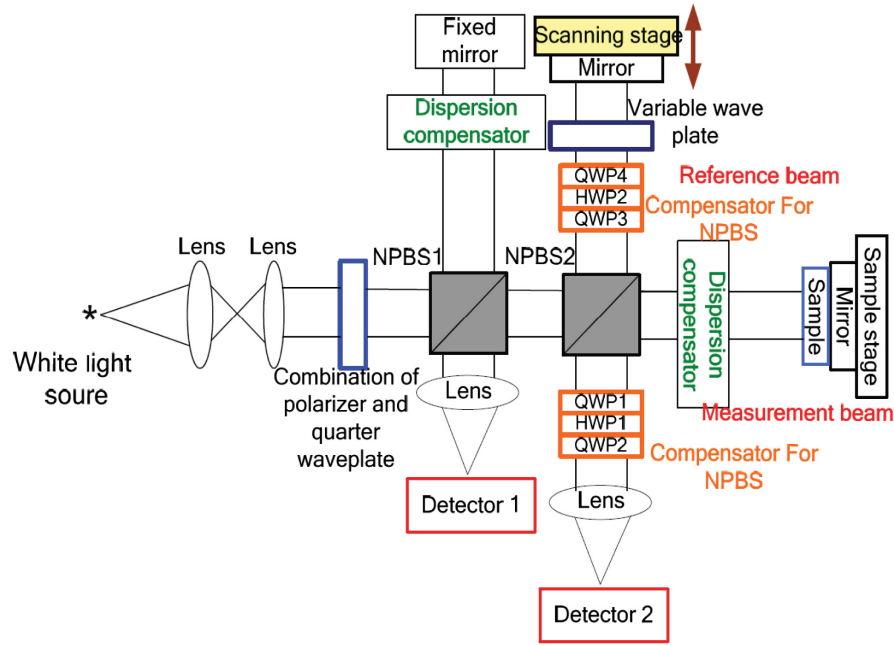


Fig. 1 Schematic illustration of proposed Mueller OCT system.²¹

applicability of the proposed method is demonstrated by measuring the optical rotation angle and depolarization index of the tissue on the fingertip of healthy human volunteers under various glucose conditions.

2 Mueller Optical Coherence Tomography System for Extraction of Circular Birefringence and Depolarization Properties of Optical Sample

Figure 1 shows the Mueller OCT measurement system used in the present study to extract the CB and depolarization (Dep)

properties of aqueous glucose solutions with scattering properties. (Note that full details of the OCT setup are presented in Ref. 21.) Briefly, however, a low-coherence interferometric signal is obtained at detectors 1 and 2 as the scanning stage is driven at a constant velocity. The signal at detector 1 is obtained by locating the peak of the envelope of the signal for extracting the thickness and refractive index of the samples, whereas the signals obtained at detector 2 are employed to determine the anisotropic properties of the sample by calculating the amplitude of the interferometric signal.

In general, the Mueller matrix of an optical sample has the form²¹

$$\mathbf{M} = \begin{bmatrix} M_{11} & M_{12} & M_{13} & M_{14} \\ M_{21} & M_{22} & M_{23} & M_{24} \\ M_{31} & M_{32} & M_{33} & M_{34} \\ M_{41} & M_{42} & M_{43} & M_{44} \end{bmatrix} = \begin{bmatrix} HH + HV + VH + VV & HH + HV - VH - VV & 2PH + 2PV - M_{11} & 2RH + 2RV - M_{11} \\ HH - HV + VH - VV & HH - HV - VH + VV & 2PH - 2PV - M_{21} & 2RH - 2RV - M_{21} \\ 2HP + 2VP - M_{11} & 2HP - 2VP - M_{12} & 4PP - 2PH - 2PV - M_{31} & 4RP - 2RH - 2RV - M_{31} \\ 2HR + 2VR - M_{11} & 2HR - 2VR - M_{12} & 4PR - 2PH - 2PV - M_{41} & 4RR - 2RH - 2RV - M_{41} \end{bmatrix}, \quad (1)$$

where H , V , P , and R denote horizontal, vertical, 45-deg linear, and right-hand circular states of polarization, respectively. Furthermore, the two digits in the polarization state notations indicate the polarization states of the measurement light beam and the reference light beam, respectively.

As shown in Fig. 2, the measurement beam passes through the beam splitter and is then incident on the sample. It is noted that the samples were stored in a 1-mm thickness quartz cuvette with an inside width of 40 mm. Following transmission through the sample, it is reflected from the mirror, transmitted back

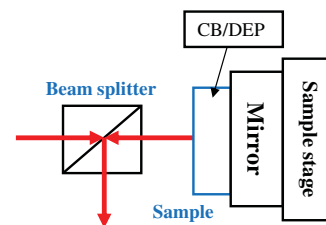


Fig. 2 Schematic diagram showing placement of sample with CB/depolarization properties in OCT system.

through the sample, and then reflected from the beam splitter. In this study, the sample with only CB/depolarization properties is studied for simplicity as associated with the glucose detection application. The optical arrangement shown in Fig. 2 can be modeled using the following Mueller matrix representation:

$$M_{CB/Dep,OCT} = M_{R,BS}M_{CB/Dep}M_{Mirror}M_{CB/Dep}M_{T,BS}, \quad (2)$$

where M_{Mirror} , $M_{T,BS}$, and $M_{R,BS}$ are the Mueller matrixes of the mirror, the beam splitter in the transmission mode, and the beam splitter in the reflection mode, respectively. (Note that all three matrixes are defined in Ref. 21.) Meanwhile, $M_{CB/Dep}$ is the Mueller matrices of the sample with CB and depolarization effects and can be expressed as

$$M_{CB/Dep} = M_{CB}M_{\Delta}, \quad (3)$$

where

$$M_{\Delta} = \begin{pmatrix} 1 & 0 & 0 & 0 \\ 0 & e^{\frac{2\eta_v^2+d_1[d_1+\sqrt{4\eta_v^2+(d_1-d_2)^2}-d_2]}{2\eta_v\sqrt{4\eta_v^2+(d_1-d_2)^2}}} & (1-e^{\frac{d_1}{\eta_v}})\eta_v & e^{\frac{1}{2}(-\eta_v-d_1-d_2)} \left[-1 - e^{\frac{\eta_v+\sqrt{4\eta_v^2+(d_1-d_2)^2}(d_1+d_2)}{2\sqrt{4\eta_v^2+(d_1-d_2)^2}}} \right] \\ 0 & (e-1)e^{\frac{d_1+\sqrt{4\eta_v^2+(d_1-d_2)^2}+d_2}{2\sqrt{4\eta_v^2+(d_1-d_2)^2}}} & \eta_v & (-1+e)e^{\frac{d_1+\sqrt{4\eta_v^2+(d_1-d_2)^2}+d_2}{2\sqrt{4\eta_v^2+(d_1-d_2)^2}}} \eta_v \\ 0 & 0 & 0 & e^{d_3} \end{pmatrix} = \begin{pmatrix} 1 & 0 & 0 & 0 \\ 0 & K_{22} & K_{23} & 0 \\ 0 & K_{32} & K_{33} & 0 \\ 0 & 0 & 0 & K_{44} \end{pmatrix}. \quad (6)$$

The depolarization index can then be calculated as

$$\Delta = \sqrt{\frac{K_{22}^2 + K_{33}^2 + K_{44}^2}{3}}. \quad (7)$$

Notably, the proposed analytical model of the sample/OCT system given in Eq. (2) allows the unknown CB and depolarization parameters of the sample to be determined over the full range, i.e., $0 < \gamma < 180$ deg and $0 < \Delta < 1$, respectively. In this proposed method, the sample is treated as a black box; thus, the physical properties of samples in a complete homogeneity are assumed. For the sake of simplicity in the signal process, only optical rotation angle and depolarization index properties of the samples were extracted. The optical rotation angle represents the CB property of glucose, whereas the depolarization index describes the scattering effect caused by scattering particles.

3 Analytical Model for Extraction of Circular Birefringence and Depolarization Properties of Turbid Media

The CB and depolarization properties of the sample can be obtained by simply equating the Mueller matrix in Eq. (1) with that given in Eq. (2). However, in practice, $M_{CB/Dep,OCT}$ is highly complex; hence, obtaining a closed-form analytical solution is extremely difficult. Accordingly, in the present study, the CB and depolarization properties of the sample are inversely derived using a genetic algorithm (GA)²⁴ with the Mueller matrix given in Eq. (1) as the target function.

$$M_{CB} = \begin{bmatrix} 1 & 0 & 0 & 0 \\ 0 & \cos(2\gamma) & \sin(2\gamma) & 0 \\ 0 & -\sin(2\gamma) & \cos(2\gamma) & 0 \\ 0 & 0 & 0 & 1 \end{bmatrix}, \quad (4)$$

in which γ is the optical rotation angle. The differential Mueller matrix describing the scattering effect in the optical sample has the form²¹

$$m_{\Delta} = \begin{bmatrix} 0 & 0 & 0 & 0 \\ 0 & -d_1 & \eta_v & 0 \\ 0 & \eta_v & -d_2 & 0 \\ 0 & 0 & 0 & -d_3 \end{bmatrix}, \quad (5)$$

where d_{1-3} are the anisotropic absorption coefficients along the x - y , 45 deg, and circular axes, respectively, and η_v is the mean value of the nondepolarizing properties. Applying a process of inverse differential calculation, the macroscopic Mueller matrix describing the scattering effect, M_{Δ} , can be obtained as

The ability of the proposed model to yield full-range measurements of the sample parameters was investigated by simulating the measured Mueller matrix using an inverse differential calculation approach given assumed parameter values for a hypothetical sample. In particular, the assumed values were input into the measured Mueller matrix, and the GA method was then used to obtain the input values inversely using the proposed analytical model.²⁴ The extracted values obtained using the GA were then compared with the theoretical input values. In other words, the accuracy of the GA extraction results was evaluated using the following fitness function:

$$F_{\text{Fitness}} = \sum_{i=1, j=1}^n \{\text{abs}[(M_{ij,\text{experiment}}^2 - M_{ij,\text{theory}}^2)]\}, \quad n = 4, \quad (8)$$

where $M_{ij,\text{experiment}}$ is the Mueller matrix given in Eq. (1) and $M_{ij,\text{theory}}$ is the Mueller matrix of the sample with CB/Dep properties in Eq. (2). The GA process commenced by generating an initial random population of candidate solutions for the depolarization matrix elements (i.e., d_1 , d_2 , d_3 , and η_v) and optical rotation angle (γ). If the resulting error between the theoretical output Mueller matrix and experimental output Mueller matrix was less than a certain target tolerance value of 10^{-5} in F_{Fitness} , the GA was terminated and the optimal values of the depolarization matrix elements and optical rotation angle or depolarization index were recovered from the corresponding candidate solution. It is noted that the target tolerance value was chosen

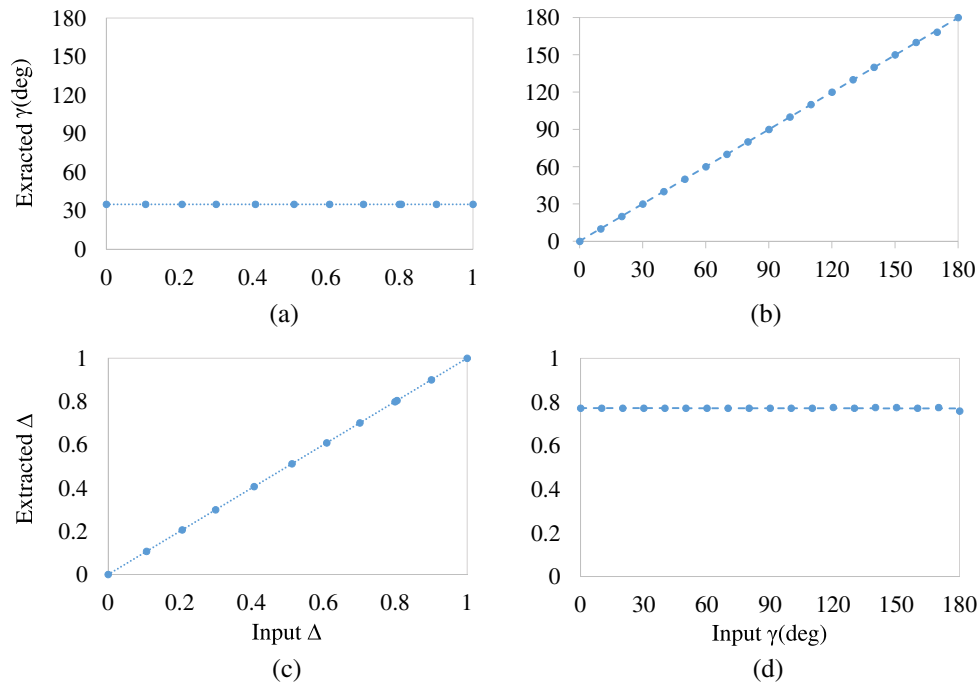


Fig. 3 Extracted values of γ and Δ for hypothetical CB/Dep sample given input values of (a) and (c) $\gamma = 35$ deg and $\Delta = 0$ to 1; and (b) and (d) $\gamma = 0$ deg to 180 deg and $\Delta = 0.77$.

to achieve the highly accurate results and minimizing calculation time.

In performing the simulations, one of the considered parameters (γ or Δ) was varied over the full range, whereas the other parameters were assigned a constant default value. The simulations commenced by setting the depolarization index equal to $\Delta = 0.77$ and extracting the values of γ given input values in the range of $\gamma = 0$ deg to 180 deg. It is noted that the value of Δ was set randomly in the range of 0 to 1 to demonstrate the extraction of depolarization index. The optical rotation angle was then set as a constant $\gamma = 35$ deg, and the depolarization index was extracted for input values in the range of $\Delta = 0$ to 1. It is noted that the value of γ was set randomly in the range of 0 deg to 180 deg for demonstrating the extraction of depolarization index. To minimize the fitness function in Eq. (8), run a loop 100 times and calculate the loop 20 times. The results of the fitness function should be set under 1×10^{-5} . It is noted that the error function in Eq. (8) is set as 10^{-2} . The extracted values of the two optical parameters with the input values in every case are shown in Fig. 3. In general, the results confirm that the CB and depolarization parameters can both be extracted over the full range, i.e., $0 < \gamma < 180$ deg and $0 < \Delta < 1$, respectively. Moreover, a good agreement is obtained between the extracted values of the optical parameters and the input values. From inspection, the standard deviations of the extracted values of γ and Δ are found to be 8.5×10^{-2} (deg) and 2.18×10^{-3} , respectively. In other words, the validity and accuracy of the GA-based analytical model are confirmed.

4 Experimental Setup and Results

As shown in Fig. 1, the OCT system consisted of a halogen lamp (R150-BM1, Techniquip, USA), two photo-detectors (2001, New Focus Corporation), a scanning stage (SGSP 20-85, Sigma Koki, Japan), a scanning stage driver (Mark-204MS, Sigma Koki, Japan), a dispersion compensator consisting of D263T

glass plate and a waveplate (5540, New Focus Corporation), an oscilloscope (6050, LeCroy Corporation), and two nonideal beam splitters (BS010, Thorlab) conducting the experiments. Compensation for the polarization distortion was performed using a composite polarizer component comprising a quarter-wave plate, half-wave plate, and second quarter-wave plate (Q/H/Q). (Note that full details of the compensation process are provided in Ref. 21.)

4.1 Parameter Extraction for Aqueous Glucose Samples with Low Scattering Effects

Aqueous glucose samples were prepared comprising deionized (DI) water mixed with glucose powder in concentrations ranging from 0 to 4000 mg/dL (in increments of 1000 mg/dL) and 0.02% Lipofundin (Lipofundin MCT/LC1 20%, B1Braun, Germany, particle size: 150 to 230 nm). The tissue phantom samples were stored in a 1-mm thickness quartz cuvette with an inside width of 40 mm. Figures 4(a) and 4(b) show the experimental results obtained for the variations of the optical rotation angle and depolarization index, respectively, with the glucose concentration. Note that, in compiling the results presented in Fig. 4, the optical rotation angle and depolarization index values obtained for an empty container were first subtracted such that the plotted results correspond to the sample only. The dash line in Fig. 4(a) shows the variation of the extracted optical rotation angle of the samples with the glucose concentration when performing the measurement process using the OCT system. As shown in Fig. 4(a), the optical rotation angle (γ) system increases approximately linearly with increases in the glucose concentration. The correlation coefficient has a value of $R^2 = 0.9101$, indicating a linearity between two variables. Furthermore, the standard deviations of the measured values of γ obtained over four repeated extractions are shown in Table 1, and the average deviation is found around 0.125 deg. Sun et al.²⁵ obtained a measurement sensitivity of approximately

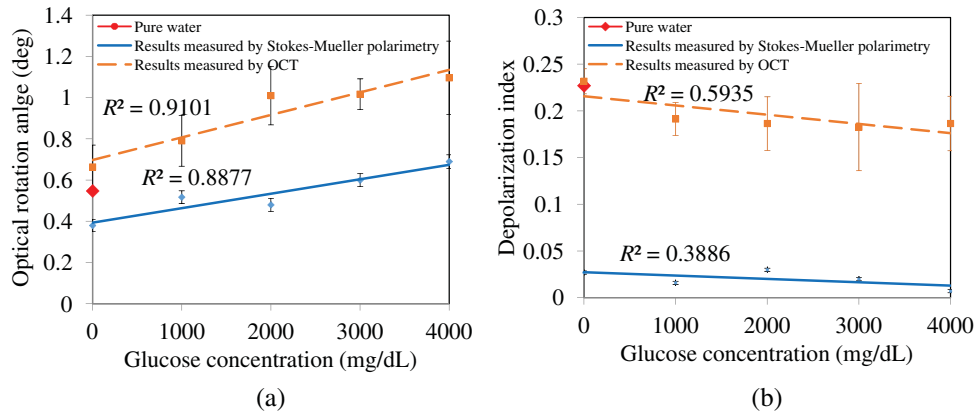


Fig. 4 Variation of (a) the optical rotation angle and (b) the depolarization index with glucose concentration for aqueous glucose samples with 0.02% Lipofundin using the OCT system and Stokes–Mueller polarimetry system.

Table 1 The standard deviations of the measured values of γ obtained on four repeated extractions over the measured concentration range of aqueous glucose samples with 0.02% Lipofundin using OCT system.

Glucose concentration	0 mg/dL	1000 mg/dL	2000 mg/dL	3000 mg/dL	4000 mg/dL	Average
γ (deg)	0.661	0.893	0.980	0.947	0.862	
	0.804	0.842	0.935	1.031	1.295	
	0.634	0.816	1.219	1.115	1.124	
	0.546	0.612	0.906	0.973	1.104	
Standard deviation (deg)	0.106	0.123	0.142	0.074	0.178	0.125

0.25 deg/(mg/dL) when measuring the glucose concentration of polystyrene sphere suspensions. Similarly, Malik and Coté²⁶ detected glucose concentration with a sensitivity of 0.04 deg/(mg/dL) over a concentration range of 0 to 600 mg/dL. The results presented in Fig. 4(a) indicate that the proposed OCT system has a measurement sensitivity of ~0.11 deg/(mg/dL). In other words, the system achieves a good sensitivity in measuring the glucose concentration. The dash line in Fig. 4(b) shows the variation of the extracted depolarization index with the glucose concentration when performing the measurement process using the OCT system. The correlation coefficient has a low value of $R^2 = 0.5993$, and it still can be seen that the depolarization index slightly reduces with increases in the glucose concentration. The present results

are thus consistent with those of previous studies,^{5–7} which showed that the depolarization index reduces with increases in the glucose concentration as a result of a corresponding increase in the refractive index and reduction in the refractive-index mismatch between the glucose solution and the Lipofundin powder. Furthermore, the standard deviations of the measured values of Δ obtained over four repeated extractions are shown in Table 2, and the average deviation is found around 0.027.

The red dots shown in Figs. 4(a) and 4(b) indicate the optical rotation angle and depolarization index, respectively, for a pure water sample obtained using the OCT system. The two parameters have values of 0.546 deg and 0.227, respectively. In theory, both parameters have a value equal to zero for pure water. Thus,

Table 2 The standard deviations of the measured values of Δ obtained on four repeated extractions over the measured concentration range of aqueous glucose samples with 0.02% Lipofundin using OCT system.

Glucose concentration	0 mg/dL	1000 mg/dL	2000 mg/dL	3000 mg/dL	4000 mg/dL	Average
Δ	0.237	0.187	0.223	0.120	0.198	
	0.241	0.185	0.156	0.227	0.220	
	0.220	0.198	0.194	0.174	0.173	
	0.216	0.157	0.172	0.207	0.153	
Standard deviation	0.012	0.017	0.128	0.046	0.292	0.027

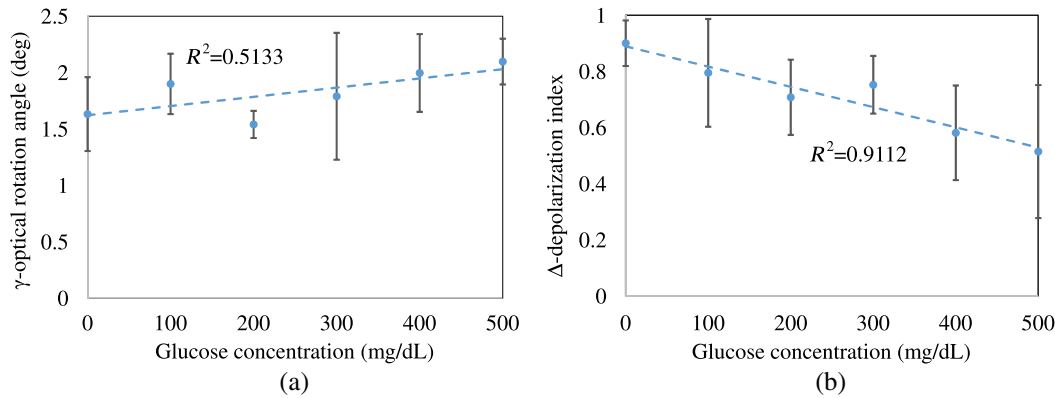


Fig. 5 Variation of (a) the optical rotation angle and (b) the depolarization index with glucose concentration for aqueous glucose samples with 2% Lipofundin.

it is speculated that the OCT system contains a small degree of experimental error due to component misalignments and imperfections of the optical elements themselves.

The solid-line in Fig. 4 shows the results obtained for the variation of the optical rotation angle and depolarization index of the samples with the glucose concentration when performing the measurement process using a transmission-mode Stokes–Mueller polarimetry system.²⁷ As for the case of the OCT, the optical rotation angle increases linearly with increases in the glucose concentration with a correlation coefficient of $R^2 = 0.8877$, whereas the depolarization index slightly reduces with increases in the glucose concentration with a correlation of $R^2 = 0.3886$. The difference between the two sets of results can be attributed to a difference in the optical path length (OPL) in the two systems. Specifically, the OPL in the Stokes–Mueller polarimetry system is much shorter than that in the OCT system. From an inspection of Fig. 4, the sensitivity of the Stokes–Mueller polarimetry system is around 0.04 deg/(mg/dL). By contrast, that of the OCT system is 0.11 deg/(mg/dL). It is noted that the large deviations and the nonlinearity of the measured results could be attributed to the misalignment of the system, the imperfections of the optic components themselves, and the noise environment.

4.2 Parameter Extraction for Tissue Phantom Samples with High Scattering Effects

Biotissue phantom samples were prepared by mixing DI water with 10-ml glucose solutions (100 mg/ml-Merck Ltd.) with concentrations 0 to 500 mg/dL (in 100 mg/dL increments) and 2% Lipofundin (Lipofundin MCT/LC1 20%, B1Braun, Germany, particle size 150 to 230 nm). Note that previous studies^{28,29} have shown that 2% of Lipofundin in solution accurately reproduces the scattering effect of human skin and tissue. Figure 5 shows the experimental results obtained for the variation of the optical rotation angle and depolarization index with the glucose concentration. As shown in Fig. 5(a), although the correlation coefficient has a value of $R^2 = 0.5133$, the optical rotation angle still slightly increases with increases in the glucose concentration. The extracted optical rotation angles for the six samples have standard deviation values of 0.327, 0.268, 0.125, 0.562, 0.344, and 0.203, respectively. Figure 5(b) shows the variation of the extracted depolarization index with the glucose concentration. It is found that the depolarization index decreases approximately linearly with increases in the glucose concentration with a value of $R^2 = 0.9112$. The standard

deviation values for the six samples are 0.081, 0.191, 0.134, 0.102, 0.168, and 0.236, respectively. The results are, therefore, in good qualitative agreement with those presented in Ref. 19. The reduction in the depolarization index with increases in the glucose concentration is to be expected as a higher glucose concentration results in a higher refractive index. As a consequence, the velocity at which light travels through the aqueous sample is reduced and, hence, the scattering effect is also reduced.

In general, the results shown in Fig. 5 confirm the feasibility of the proposed OCT system for performing glucose sensing based on just two optical parameters. The optical rotation angle represents the CB property of the glucose sample, whereas the depolarization index represents the scattering effects caused by particles within the sample. In general, the depolarization index reduces as a result of the OPL traversed by the light in passing through the sample. Therefore, both parameters (i.e., the optical rotation angle and the depolarization index) are required to obtain reliable estimates of the glucose concentration.

4.3 Glucose Extraction on Human Fingertip

The practical feasibility of the proposed optical system was evaluated by measuring the optical rotation angle and depolarization index of the tissue on the fingertips of healthy human volunteers. The experiments commenced by measuring the optical rotation angle and depolarization index of four volunteers under two glucose conditions, namely before and after an enhanced glucose condition induced by drinking 700 mL of sugared water. Note that in the latter case, glucose detection was performed 15 min after the drink was consumed to allow

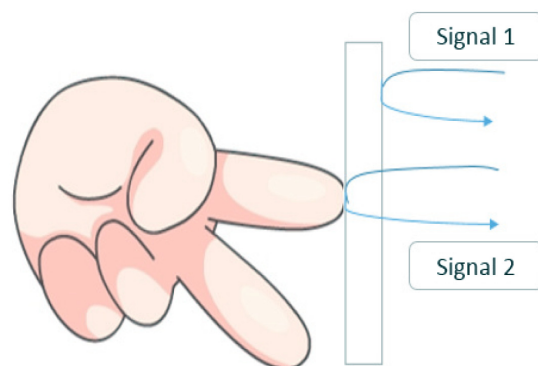


Fig. 6 The illustration of human fingertip experiment.

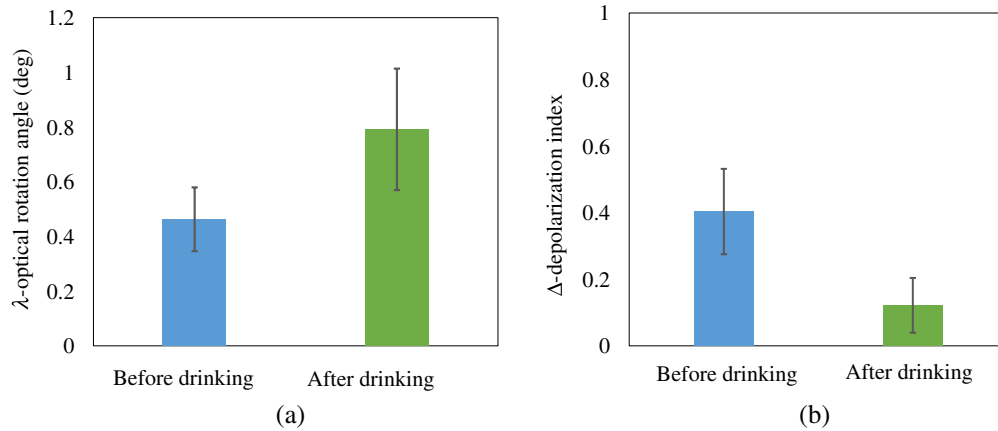


Fig. 7 Average values of (a) optical rotation angle and (b) depolarization index of fingertip of subject #1 under different glucose conditions.

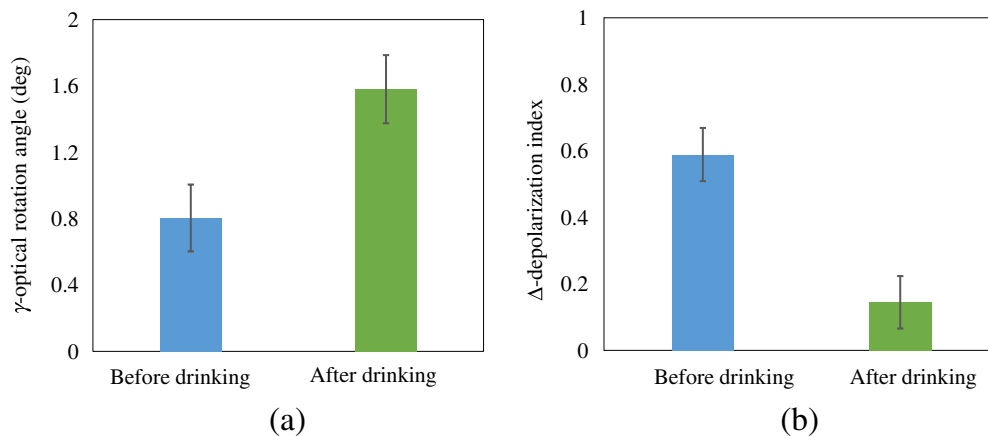


Fig. 8 Average values of (a) optical rotation angle and (b) depolarization index of fingertip of subject #2 under different glucose conditions.

sufficient time for the sugar to enter the bloodstream. In performing the experiments, the volunteer's fingertip was pressed against a 1-mm-thickness glass plate as shown in Fig. 6.

Furthermore, for both glucose conditions for each subject, four glucose measurements were obtained over a period of 20 min. The experimental results obtained for the four subjects are shown in Figs. 7–10. For all of the subjects other than subject

#3, the average optical rotation angle increased following ingestion of the sugared water. Moreover, the average depolarization index reduced in every case. In other words, the results are in good agreement with those presented in Fig. 5(a) for the tissue phantom samples. It is noted that the strict preparation of volunteers for glucose testing is extremely necessary due to the different results obtained for subject #3.

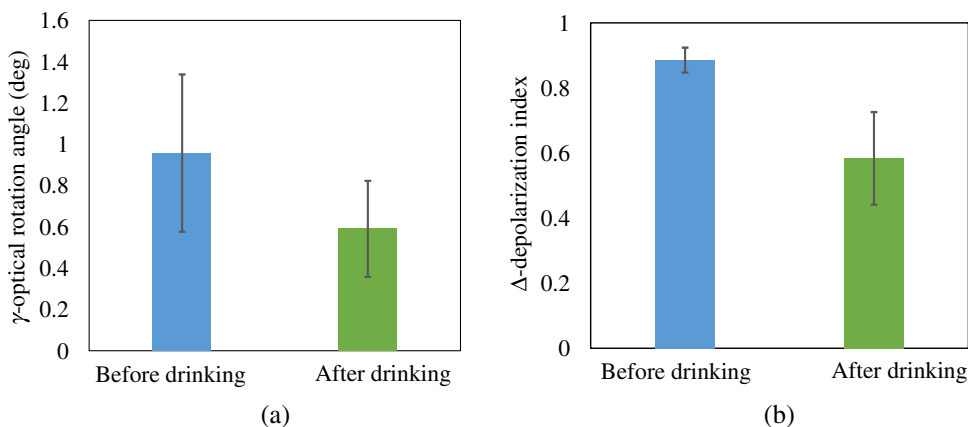


Fig. 9 Average values of (a) optical rotation angle and (b) depolarization index of fingertip of subject #3 under different glucose conditions.

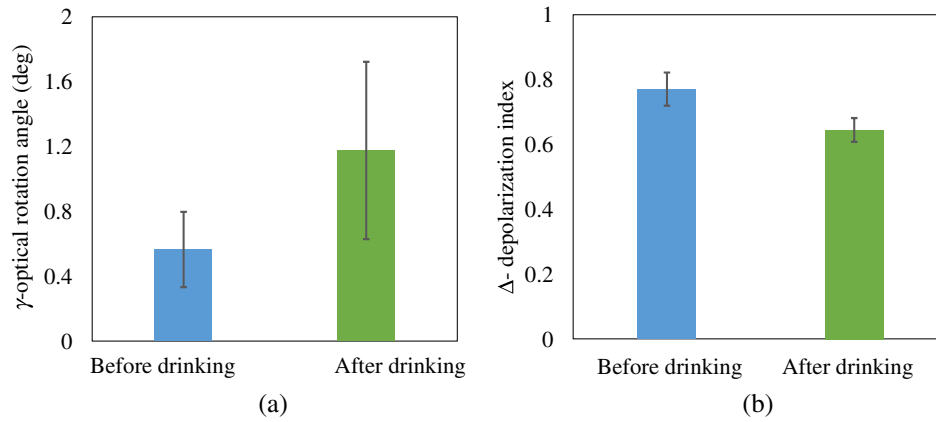


Fig. 10 Average values of (a) optical rotation angle and (b) depolarization index of fingertip of subject #4 under different glucose conditions.

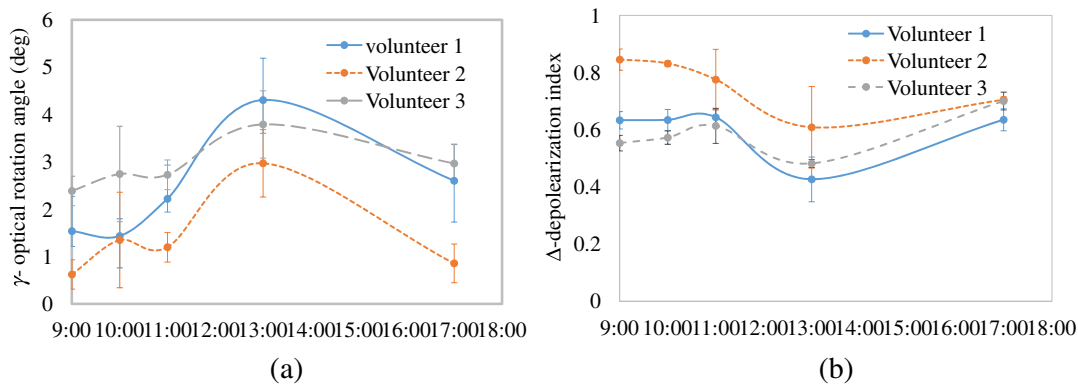


Fig. 11 Extracted values of (a) optical rotation angle and (b) depolarization index of fingertips of three volunteers at five different times of the day.

A second series of experiments was performed in which the fingertip glucose concentration was measured for three volunteers at five different times over an 8-h period. The times were chosen in such a way as to track natural variations in the glucose concentration due to ingestion of food and drink at mealtimes, i.e., 9:00 AM (before breakfast), 10:00 AM (after breakfast), 11:00 AM (before lunch), 13:00 PM (after lunch), and 17:00 (before dinner). As in the previous experiments, the measurement process was performed using a 1-mm-thick glass attached to the fingertip. Four glucose measurements were obtained over a 20-min period in each case. Figures 11(a) and 11(b) show the extraction results obtained for the optical rotation angle and depolarization index of the three volunteers at the five different measurement times. As shown in Fig. 11(a), the optical rotation angle increased following breakfast (except for the case of volunteer 1) and, following a slight dip at 11:00 AM, increased to a peak value after lunch before decreasing continuously until 17:00 PM. Conversely, Fig. 11(b) shows that the depolarization index increased before meal times (indicating a lower glucose concentration) and decreased after the meal times (indicating a higher glucose concentration). In other words, the results are again in good qualitative agreement with those obtained for the tissue phantom sample [Fig. 5(b)]. Moreover, the standard deviations of the γ and Δ measurements obtained at five different times over an 8-h daytime period are equal to 0.302 deg and 0.045, respectively.

5 Conclusions

This study has presented a Mueller OCT system for evaluating the glucose concentration of aqueous samples by means of two optical parameters (the optical rotation angle and the depolarization index) extracted using a differential Mueller model. The basic feasibility of the proposed method has been demonstrated by extracting the optical rotation angle and depolarization index of aqueous glucose solutions containing glucose with concentrations of 0 to 4000 mg/dL and 0.02% Lipofundin powder. The results have shown that the optical rotation angle increases, whereas the depolarization index decreases, with increases in the glucose concentration. A similar tendency has been found for tissue phantom samples containing 2% Lipofundin powder. The practical applicability of the proposed method has been demonstrated by measuring the optical rotation angle and depolarization index of the human tissue on the fingertips of three healthy volunteers before and after the ingestion of sugared water, respectively. Moreover, the standard deviations of the γ and Δ measurements obtained at five different times over an 8-h daytime period are equal to 0.302 deg and 0.045, respectively. The results obtained for human tissue are in a good qualitative agreement with those obtained for phantom tissue samples. Hence, the basic feasibility of the proposed OCT system for noninvasive glucose monitoring is confirmed. In the future, Monte Carlo theory will be implemented into the model to obtain the quantitative predictions of the glucose

concentration from the experimentally extracted values of the optical rotation angle and depolarization index. Thus, the scattering properties of different people with different ages, race, and skin color will be investigated and studied in more detail to achieve trustable results for glucose concentration extraction.

Disclosures

No conflicts of interest, financial or otherwise, are declared by the authors. The current study has followed our institutional policies for the use of human subjects in our research. The informed consent was waived by the oversight body.

Acknowledgments

The authors gratefully acknowledge the financial support provided to this study by the Ministry of Science and Technology (MOST) of Taiwan under Grant No. NSC 106-2221-E-006-020-MY2. This research was also supported in part by the Ministry of Education, Taiwan, under the "Aim for Top University Project" of National Cheng Kung University.

References

1. L. Guariguata et al., "The international diabetes federation diabetes atlas methodology for estimating global and national prevalence of diabetes in adults," *Diabetes Res. Clin. Pract.* **94**, 322–332 (2011).
2. O. S. Khalil, "Non-invasive glucose measurement technologies: an update from 1999 to the dawn of the new millennium," *Diabetes Technol. Ther.* **6**, 660–697 (2004).
3. K. Song et al., "An impedance and multi-wavelength near infrared spectroscopy IC for noninvasive blood glucose estimation," *IEEE J. Solid-State Circuits* **50**, 1025–1037 (2015).
4. D. Coté and I. A. Vitkin, "Balanced detection for low noise precision measurements of optically active, multiply scattering tissue phantoms," *J. Biomed. Opt.* **9**, 213–220 (2004).
5. M. J. S. Timmerman et al., "Raman spectroscopy as a promising tool for noninvasive point-of-care glucose monitoring," *J. Diabetes Sci. Technol.* **8**, 974–979 (2014).
6. J. T. Bruulsema et al., "Correlation between blood glucose concentration in diabetics and noninvasively measured tissue optical scattering coefficient," *Opt. Lett.* **22**, 190–192 (1997).
7. J. S. Maier et al., "Possible correlation between blood glucose concentration and the reduced scattering coefficient of tissues in the near infrared," *Opt. Lett.* **19**, 2062–2064 (1994).
8. M. Kohl, M. E. Matthias, and M. Cope, "The influence of glucose concentration upon the transport of light in tissue-simulating phantoms," *Phys. Med. Biol.* **40**, 1267–1287 (1995).
9. A. Popov, A. Priezzhev, and R. Myllyla, "Effect of glucose concentration in a model light-scattering suspension on propagation of ultrashort laser pulses," *Quantum Electron.* **35**, 1075–1078 (2005).
10. E. Alarousu et al., "Non-invasive glucose sensing in scattering media using OCT, PAS and TOF techniques," *Proc. SPIE* **5474**, 33–41 (2003).
11. A. Popov et al., "Glucose sensing in flowing blood and intralipid by laser pulse time-of-flight and optical coherence tomography techniques," *IEEE J. Sel. Top. Quantum Electron.* **18**, 1335–1342 (2012).
12. R. O. Esenaliev, K. V. Larina, and M. Motamedi, "Noninvasive monitoring of glucose concentration with optical coherence tomography," *Opt. Lett.* **26**, 992–994 (2001).
13. K. V. Larin et al., "Noninvasive blood glucose monitoring with optical coherence tomography: a pilot study in human subjects," *Diabetes Care* **25**, 2263–2267 (2002).
14. K. V. Larin et al., "Specificity of noninvasive blood glucose sensing using optical coherence tomography technique: a pilot study," *Phys. Med. Biol.* **48**, 1371–1390 (2003).
15. M. Y. Kirillin et al., "Glucose sensing in aqueous intralipid suspension with an optical coherence tomography system: experiment and Monte Carlo simulation," *Proc. SPIE* **5325**, 164–173 (2004).
16. C. K. Hitzberger et al., "Measurement and imaging of birefringence and optic axis orientation by phase resolved polarization sensitive optical coherence tomography," *Opt. Express* **9**, 780–790 (2001).
17. J. F. D. Boer et al., "Two dimensional birefringence imaging in biological tissue by polarization sensitive optical coherence tomography," *Opt. Lett.* **22**, 934–936 (1997).
18. M. R. Hee et al., "Polarization sensitive low coherence reflectometer for birefringence characterization and ranging," *J. Opt. Soc. Am. B* **9**, 903–908 (1992).
19. G. Yao and L. V. Wang, "Two dimensional depth resolved Mueller matrix characterization of biological tissue by optical coherence tomography," *Opt. Lett.* **24**, 537–539 (1999).
20. S. Jiao, G. Yao, and L. V. Wang, "Depth resolved two dimensional Stokes vectors of backscattered light and Muller matrices of biological tissue measured with optical coherence tomography," *Appl. Opt.* **39**, 6318–6324 (2000).
21. C. C. Liao and Y. L. Lo, "Extraction of linear anisotropic parameters using optical coherence tomography and hybrid Mueller formalism," *Opt. Express* **23**, 10653–10667 (2015).
22. B. Kunnen et al., "Application of circularly polarized light for non-invasive diagnosis of cancerous tissues and turbid tissue-like scattering media," *J. Biophotonics* **8**, 317–323 (2015).
23. Q. H. Phan and Y. L. Lo, "Differential Mueller matrix polarimetry technique for noninvasive measurement of glucose concentration on human fingertip," *Opt. Express* **25**, 15179–15187 (2017).
24. T. C. Yu and Y. L. Lo, "A novel heterodyne polarimeter for the multiple parameter measurements of twisted nematic liquid crystal cell using a genetic algorithm approach," *J. Lightwave Technol.* **25**, 946–951 (2007).
25. P. Sun et al., "Mueller matrix decomposition for determination of optical rotation of glucose molecules in turbid media," *J. Biomed. Opt.* **19**, 046015 (2014).
26. B. H. Malik and G. L. Coté, "Modeling the corneal birefringence of the eye toward the development of a polarimetric glucose sensor," *J. Biomed. Opt.* **15**, 037012 (2010).
27. Q. H. Phan and Y. L. Lo, "Stokes–Mueller matrix polarimetry system for glucose sensing," *Opt. Lasers Eng.* **92**, 120–128 (2017).
28. R. Ankri et al., "Intercoupling surface plasmon resonance and diffusion reflection measurements for real-time cancer detection," *J. Biophotonics* **6**, 188–196 (2013).
29. T. L. Troy and S. N. Thennadil, "Optical properties of human skin in the near infrared wavelength range of 1000 to 2200 nm," *J. Biomed. Opt.* **6**, 167–176 (2001).

Tseng-Lin Chen received his BS degree in mechanical engineering from National Cheng Kung University, Tainan, Taiwan, R.O.C. His research interests include OCT for biosensing.

Yu-Lung Lo received his BS degree from National Cheng Kung University, Tainan, Taiwan, ROC, in 1985, and his MS degree and PhD in mechanical engineering from the Smart Materials and Structures Research Center, University of Maryland, USA, in 1992 and 1995, respectively. Currently, he is the chairman of the Asian Society of Experimental Mechanics (ASEM) and the Steering Committee in International Symposium on Optomechatronics Technology (ISOT). His research interests include experimental mechanics, fiber-optic sensors, optical techniques in precision measurements, biophotonics, and additive manufacturing. He has authored over 150 journal publications, and one article was included in Spotlight on Optics by OSA in 2015.

Chia-Chi Liao received his PhD in mechanical engineering from National Cheng Kung University, Tainan, Taiwan, R.O.C. His research interests include OCT for biosensing.

Quoc-Hung Phan received his BS degree in mechanical engineering from HCM University of Technology, Viet Nam in 2004 and his MS degree in Department of Mechanical Engineering at Southern Taiwan University, Tainan, Taiwan, R.O.C. In 2016, he received his doctor's degree in the Department of Mechanical Engineering, National Cheng Kung University. His research interests include subwavelength sensors, polarimetry, and optical biosensing.